Transmission Line Modeling of Coupled Lines in a Semiconducting Substrate

Daniël De Zutter and Thomas Demeester

***Abstract*—This paper briefly describes some aspects of transmission line modeling. In particular some issues related to the most general case of multiconductor lines on a semiconducting substrate are adressed, and a number of examples illustrate the possibilities of the developed model.**

***Index Terms*—Transmission line modeling, semiconducting substrate, surface admittance, RLGC-parameters.**

I. Multiconductor Lines and Transmission Line Analysis

THE general problem of multiconductor lines embedded in (planar) layered substrates has been abundantly treated in literature and in a large number of books. The analysis starts from the transversal cross-section, usually taken to be the (x, y)-plane, and the structure is supposed to remain invariant along the longitudinal signal propagation direction (the z-axis). Solving the source-free Maxwell's equations under the above assumptions leads to an eigenmode analysis. In the sinusoidal regime the typical signal propagation dependency of each mode becomes $\cos(\omega t - \beta z + \phi)$ for a signal propagating along the positive z-axis, with $\omega = 2\pi f$ and f the frequency, and with $\beta(\omega)$ the (in general complex) frequency-dependent wavenumber of one of the modes that can be sustained by the multiconductor lines. As noted before many different configurations have been studied in literature with layered, isotropic or (bi)anisotropic substrate materials, lossless and lossy dielectrics, semi-conductors etc. For additional information we refer the reader e.g. to [1]. Finding eigenmodes and wavenumbers (eigenvalues) is only one aspect of the problem. As the multiconductor lines are part of a complete interconnection (in a cable, on a board, in a package, on chip, ...) it is important to obtain an $\mathsf{R}, \mathsf{L}, \mathsf{G}, \mathsf{C}$ description. These familiar resistance, inductance, conductance and capacitance matrices allow to describe the behaviour of the multiconductor system by the so-called Telegrapher Equations:

$$\frac{\partial \mathbf{i}(\omega, z)}{\partial z} = -(j\omega\mathsf{C} + \mathsf{G})\ \mathbf{v}(\omega, z) \quad (1)$$

$$\frac{\partial \mathbf{v}(\omega, z)}{\partial z} = -(j\omega\mathsf{L} + \mathsf{R})\ \mathbf{i}(\omega, z) \quad (2)$$

Here $\mathbf{v}(\omega, z)$ and $\mathbf{i}(\omega, z)$ are $N \times 1$ column vectors formed by the voltages and total currents associated with each conductor (the complete system consist of $N + 1$ conductors, one of which has been taken as the reference conductor). The whole discussion now boils down to the way in which physical (and/or mathematical) meaning can be given to these voltages and currents and to the circuit parameters and how to express them in terms of the fields. In literature several ways to deal with this problem have been explored and discussed. At low frequencies voltages and currents can be defined in a completely consistent way. When frequencies increase, however, this is no longer the case. Definitions can then be based on, e.g., (partial) power conservation, reciprocity conservation or causality conservation. In all those cases one can either choose the current as the quantity to which a clear physical meaning is given (as is most often the case for conductors), or the voltage (e.g. for slotline analysis). In general it is no longer possible to give a clear physical meaning to both voltage and current. Moreover, the circuit parameters, i.e. the transmission line equivalent, will differ when adopting the different techniques. In our presentation we will give some more details on this aspect of the problem

The authors are with the Department of Information Technology, Ghent University, Ghent, Belgium. E-mail: daniel.dezutter@ugent.be, thomas.demeester@ugent.be.

II. Multiconductor Lines in Semiconducting Substrates

This particular problem is very challenging due to the large influence of the semi-conducting substrate on the circuit parameters when the frequency varies from DC to about 100 GHz, when considering the still relevant harmonics in the transmitted bits. Of special importance is a possible slow-wave phenomenon meaning that in a particular frequency band signals propagate (much) slower, leading to an important bit distortion. A thorough analysis of a single conductor line embedded in a semiconducting substrate and an overview of related work are presented in [2] revealing the presence of dielectric, slow-wave and skin-effect modes. In this presentation we will discuss how this analysis can be extended to the multiconductor case. The problem is basically tackled by replacing the considered configuration by an equivalent one consisting of well-chosen surface charges and surface currents. These charges and currents depend, respectively, on the electric potential and on the longitudinal electric field. These relationships are expressed using the surface admittance concepts first put forward in [3]. We will also give some details on this in the oral presentation with special attention devoted to the meaning of voltages, current and the RLGC-parameters. Because mode orthogonality plays a crucial role in the extension from the single conductor to the multiple conductor case, it turns out to be "natural" to use the reciprocity conservation principle to derive a transmission line equivalent. The surface admittance concepts also allow to extend the analysis to other configurations such as coated conductors (which are of importance for on chip interconnects), still retaining a very high precision when predicting the skin-effect and current crowding over a very large frequency band.

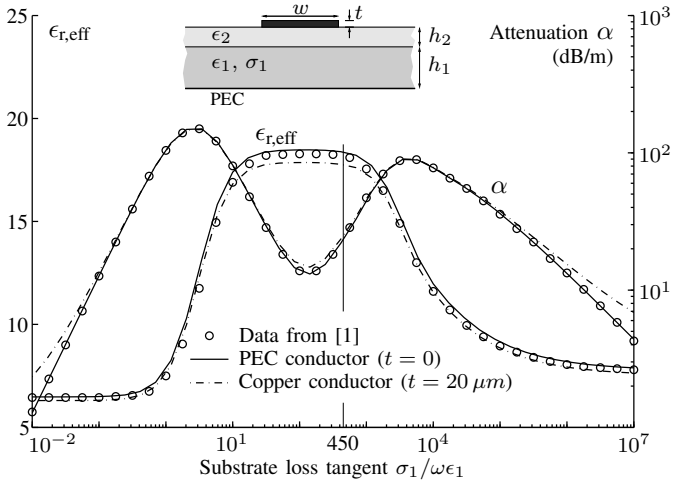

Fig. 1. Effective relative permittivity $\epsilon_{r,eff}$ and attenuation coefficient (dB/m) for the fundamental mode of the shown MIS microstrip line at 1 GHz, as a function of the loss tangent $\sigma_1/\omega\epsilon_1$ of the lower substrate. $w = 600\,\mu m$, $h_1 = 500\,\mu m$, $h_2 = 135\,\mu m$, and $\epsilon_1 = \epsilon_2 = 9.7\,\epsilon_0$. The vertical line indicates where $\sigma_1 = 450\,\omega\epsilon_1$.

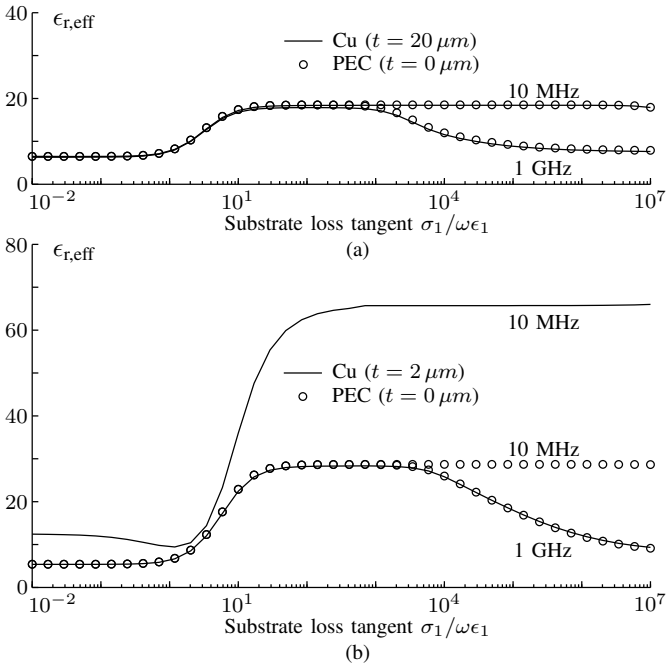

Fig. 2. $\epsilon_{r,eff}$ at 10 MHz and 1 GHz for (a) the configuration as in Fig. 1 ($h_1 = 500\,\mu m$, $h_2 = 135\,\mu m$, $w = 600\,\mu m$), and (b) a modified configuration with smaller conductor ($h_1 = 500\,\mu m$, $h_2 = 13.5\,\mu m$, $w = 60\,\mu m$)

Based on the above principles a code was implemented capable of handling a large variety of configurations, some examples of which are discussed below.

III. Examples

The following paragraphs with examples are merely excerpts from [4] and [5], where a more extensive discussion and additional examples can be found.

A. MIS Microstrip Line (Excerpt from [4])

As a first example, consider the open MIS microstrip line, shown on the inset of Fig. 1. The line consists of a $h_1 = 500\,\mu m$ thick lossy substrate with conductivity σ_1, separated from a thin signal conductor by a lossless dielectric layer with thickness $h_2 = 135\,\mu m$. All materials are non-magnetic (as will be the case in all the examples). Simulations were performed at 1 GHz, for increasing values of σ_1, such that the fundamental mode evolves from a dielectric mode, over the slow-wave range, to a skin effect mode. In [2], an infinitely thin and perfect electric conducting (PEC) signal line was used. Our simulation of the PEC line (full line in Fig. 1) yields identical results for the attenuation constant α. Yet, a small difference in the effective relative permittivity $\epsilon_{r,eff}$ is noticeable because the results shown here were obtained by leaving away the top side of the box surrounding the structure in [2], resulting in a small shift of the inductance and hence the observed difference in $\epsilon_{r,eff}$. The difference is very small though, and the large box described in [2] allows a good approximation of the open line structure. Simulating the signal line as a copper conductor ($\sigma_{Cu} = 58\,MS/m$) of the same width and with finite thickness ($w = 600\mu m$, $t = 20\,\mu m$) only slightly affects the results, as shown in Fig. 1 (dash-dot lines).

As an illustration of the frequency-dependency, the same configuration was simulated both for the PEC and the copper signal line, at the frequencies 10 MHz and 1 GHz. Fig. 2(a) shows that the resulting $\epsilon_{r,eff}$-values are very similar, be it that at 10 MHz the skin effect mode is never reached (current crowding would only occur for a loss tangent, higher than 10^7). In both cases, there is virtually no difference in $\epsilon_{r,eff}$ between the copper and the PEC conductor. However, now consider an analogous configuration, but with a smaller conductor, closer to the substrate ($h_2 = 13.5\,\mu m$, $w = 60\,\mu m$, and $t = 2\,\mu m$ for the copper strip). The thickness of the lower substrate and the material parameters remain unchanged. Fig. 2(b) shows that at 1 GHz, the finite conductivity of the line still has no influence on the propagation constant. The main difference between both configurations at 1 GHz, is the different value of $\epsilon_{r,eff}$ in the slow-wave range of the fundamental mode. In Fig. 2(b), $\epsilon_{r,eff}$ at 1 GHz is higher than in Fig. 2(a), because the lower substrate has a higher internal inductance (as it was not scaled together with the line), whereas the capacitance remains unchanged as soon as $\sigma_1 > \omega\epsilon_1$. At 10 MHz, $\epsilon_{r,eff}$ is much larger in Fig. 2(b) than in Fig. 2(a), although only for the copper conductor. By decreasing the dimensions of the line, the resistance R increases with respect to the inductance L and the point where $R \approx \omega L$ shifts towards higher frequencies. At 10 MHz the line in Fig. 2(b) operates in the so-called *RC-range* ($R > \omega L$).

B. Coated Conductor (Excerpt from [5])

As a second example, the coated conductor shown in Fig. 3 is modeled. The circuit inductance and resistance p.u.l. presented in Fig. 4 show that the RL-behavior of the coated conductor is quite different from that of a homogeneous copper conductor with the same dimensions. For skin-effect frequencies, the resistance increases more rapidly for the

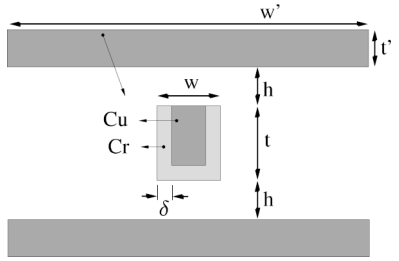

Fig. 3. Transmission line system with two copper reference conductors and a coated signal conductor (inside: Cu with resistivity ρ_{Cu}= 1.7 $\mu\Omega$cm; coating: Cr with ρ_{Cr}= 12.9 $\mu\Omega$cm). The dimensions are: w = 238, t = t' = 500, h = 450, w' = 3117, δ = 10, all in nanometers.

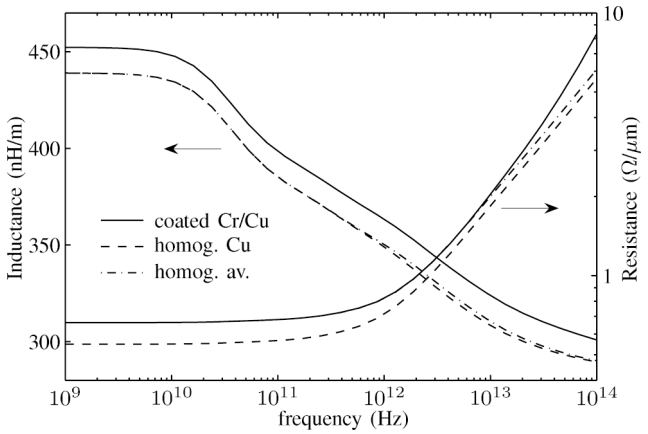

Fig. 4. Resistance and Inductance p.u.l. for the configuration of Fig. 3.

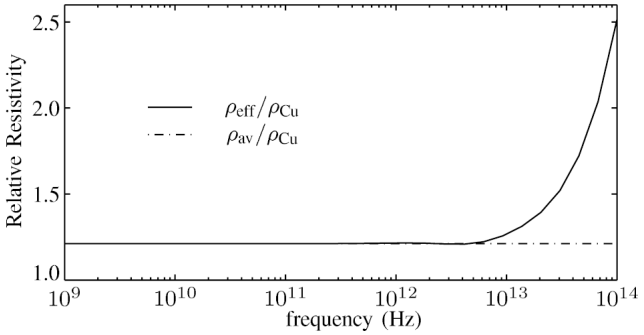

Fig. 5. Relative resistivities $\rho_{\text{eff}}/\rho_{\text{Cu}}$ and $\rho_{\text{av}}/\rho_{\text{Cu}}$, producing the resistance, resp. only the DC-resistance of the coated conductor of Fig. 3.

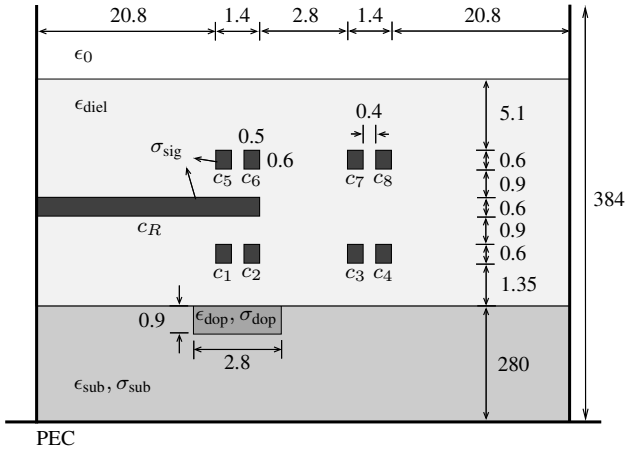

Fig. 6. Cross-section of the multi-conductor line structure of Example III-C. All indicated dimensions are in micrometers.

coated conductor, given that a gradually larger part of the current flows within the less conducting coating. A better approximation for the actual resistance is obtained by a homogeneous conductor with a resistivity ρ_{av} = 2.06 $\mu\Omega$cm, found as the weighted average of ρ_{Cu} and ρ_{Cr} such that the same DC-resistance as the coated conductor is obtained.

The configuration of Fig. 3 was taken from [6], in which a substitution of the composite conductor by a homogeneous conductor with an unknown *effective resistivity* ρ_{eff} is proposed. With the developed techniques it is now possible to actually calculate $\rho_{\text{eff}}(f)$. Fig. 5 shows this effective value as a function of frequency normalized on ρ_{Cu}. For low frequencies ρ_{eff} coincides with ρ_{av} as defined above. The difference between ρ_{eff} and ρ_{av} at higher frequencies clearly illustrates the effect of the coating. The DC-value ρ_{av} is a good approximation for $\rho_{\text{eff}}(f)$, up to the frequencies at which the skindepth $\sqrt{\rho_{\text{av}}/\pi\mu_0 f}$ becomes comparable with the coating thickness, which is far beyond the relevant frequencies in current chip technologies.

C. Multi-Conductor Line Structure (Excerpt from [4])

In the final example of Fig. 6, a transmission line system of 8 coupled lines is analyzed. The dimensions are based on a currently used semiconductor technology. Four identical pairs of conductors (c_1 to c_8) and a reference conductor (c_R), all with conductivity $\sigma_{\text{sig}} = 40\,MS/m$, are embedded in a dielectric layer above a thick semiconducting substrate, on top of a PEC plane. The substrate conductivity $\sigma_{\text{sub}} = 2\,S/m$, unless indicated differently (as for Fig. 8 and 9). Locally (underneath c_1 and c_2), the substrate has been heavily doped ($\sigma_{\text{dop}} = 0.03\,MS/m$). Permittivities are $\epsilon_{\text{diel}} = 4\epsilon_0$ and $\epsilon_{\text{sub}} = 12\epsilon_0$. The dimensions, in micrometers, are indicated in the cross-section (not shown in proportion). The structure is enclosed between two PEC 'mirror' walls at the left and right side, in order to imitate a wide slab (as was done in [2] as well).

In Fig. 7, the modal voltages on each signal conductor are presented for the 8 fundamental modes, at a frequency of 10 GHz and for a substrate conductivity $\sigma_{\text{sub}} = 2\,S/m$. For a clear graphical presentation of the modes, each normalized modal voltage V is presented with a modified amplitude $V_0 = |V| \cdot sign\big(Re(V)\big)$ and a phase ϕ, such that $V = V_0\, e^{-j\phi}$. The modes fall apart into two groups: the modes (m_1-m_4), in which both conductors of each pair have more or less the same excitation, and those (m_5-m_8), with an opposite excitation of both conductors of each pair. In the next paragraphs, they are resp. called the *even* and the *odd* modes.

The behavior of the SWF and attenuation as a function of the substrate loss factor $\sigma_{\text{sub}}/\omega\epsilon_{\text{sub}}$ is shown in Fig. 8. There is a large difference in the behavior of the even and the odd modes, which can be explained as follows. Each pair can roughly be approximated as a symmetric line pair in its own respect. For such a line, the two fundamental modes β_{even} and

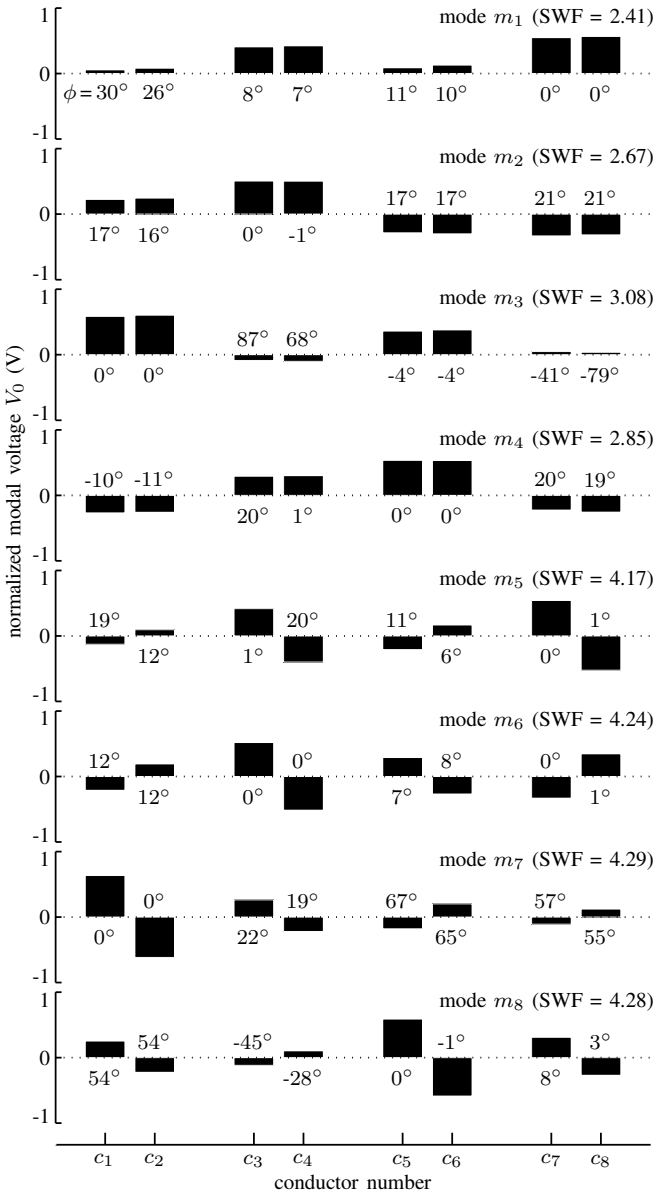

Fig. 7. Modal voltages for the configuration of Fig. 6, at 10 GHz, and with $\sigma_{\text{sub}} = 2\,S/m$. The complex modal voltages V are found as $V = V_0\, e^{-j\phi}$, with V_0 shown as bars and ϕ (expressed in degrees) at the corresponding bar. The modes can be split up into a quasi 'even' excitation of each of the conductor pairs (mode m_1 to m_4), and a quasi 'odd' excitation (mode m_5 to m_8). For each mode, the SWF is indicated as well.

β_{odd} are found from

$$\begin{aligned} \beta^2_{even} &= -\big(j\omega(C_s - |C_m|) + (G_s + G_m)\big) \\ &\quad \cdot \big(j\omega(L_s + L_m) + (R_s + R_m)\big) \\ \beta^2_{odd} &= -\big(j\omega(C_s + |C_m|) + (G_s - G_m)\big) \\ &\quad \cdot \big(j\omega(L_s - L_m) + (R_s - R_m)\big) \end{aligned} \tag{3}$$

in which the indices s and m denote the diagonal, resp. the off-diagonal elements from the (2×2) circuit matrices associated with each line pair. As an illustration, Fig. 9 shows the relevant elements of the complex matrices $\tilde{\mathsf{C}}$ and $\tilde{\mathsf{L}}$, associated with the conductor pair c_3-c_4. The elements C_{33} and C_{44} correspond to C_s from (3) (the small difference between them due to

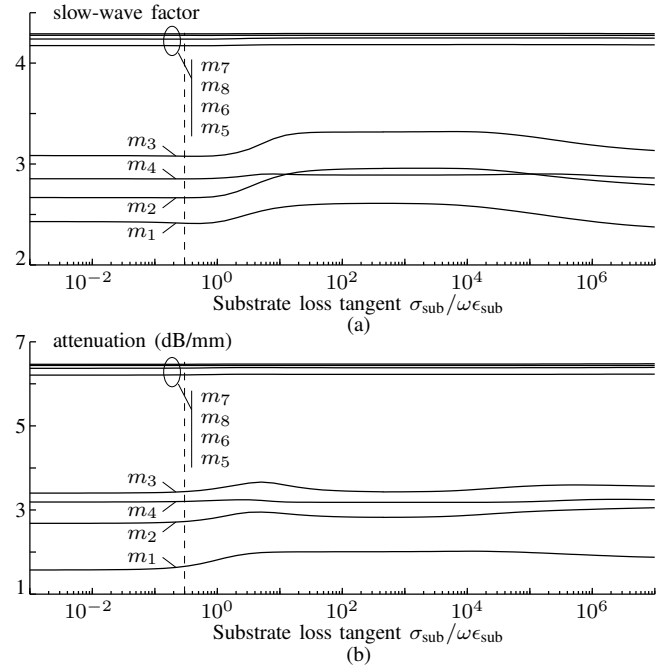

Fig. 8. Slow-wave factor (a) and attenuation constant (b) for each of the fundamental modes of the multi-conductor structure of Fig. 6 at 10 GHz, as a function of the substrate loss tangent (ranging from 10^{-3} to 10^{7}). The vertical dashed lines indicate where $\sigma_{\text{sub}} = 2\,S/m$, i.e. for which the modal voltages are shown in Fig. 7.

the actual non-symmetry of the configuration), whereas C_{34} corresponds to C_m. From Fig. 9(a), it becomes clear that the factor $(j\omega C_s + G_s)$ in (3) is dominated by the capacitance term and the numerical results confirm this is also the case for the other line pairs. For all line pairs, both C_s (positive) and C_m (negative) are influenced in the same way by the charge on the substrate's surface. As soon as the loss tangent becomes larger than about 1, an increasing σ_{sub} increases C_s, whereas $|C_m|$ decreases. For the odd mode, depending on $C_s + |C_m|$, the influence of σ_{sub} is cancelled out, whereas it is reinforced for the even mode. This explains the flat behavior of the SWF in Fig. 8(a) around $\sigma_{\text{sub}}/\omega\epsilon_{\text{sub}} \approx 1$ for the odd modes, and the increase for the even modes. This effect is not very pronounced for mode m_4, although an 'even' mode. This is due to the reference conductor, shielding c_5 and c_6 from the substrate. The reason why m_3 has the highest and m_1 the lowest SWF from the even modes, is readily explained as well. The influence of the reference conductor and the doped part (σ_{dop}) in the substrate lead to higher capacitance elements associated with the conductors on the left (c_1, c_2, c_5 and c_6, strongly excited in mode m_3) than for those on the right (excited in mode m_1). At higher values of σ_{sub}, when the magnetic field can no longer fully penetrate the substrate, an analogue argumentation based on the inductance and resistance coefficients, explains the different σ_{sub}-dependence of the odd and the even modes.

Fig. 8 also shows that the overall odd mode SWF is higher than for the even modes. As both conductors of each pair are close to one another, $|C_m|$ is of the same order of magnitude as C_s and $(C_s + |C_m|)$ is hence considerably larger than

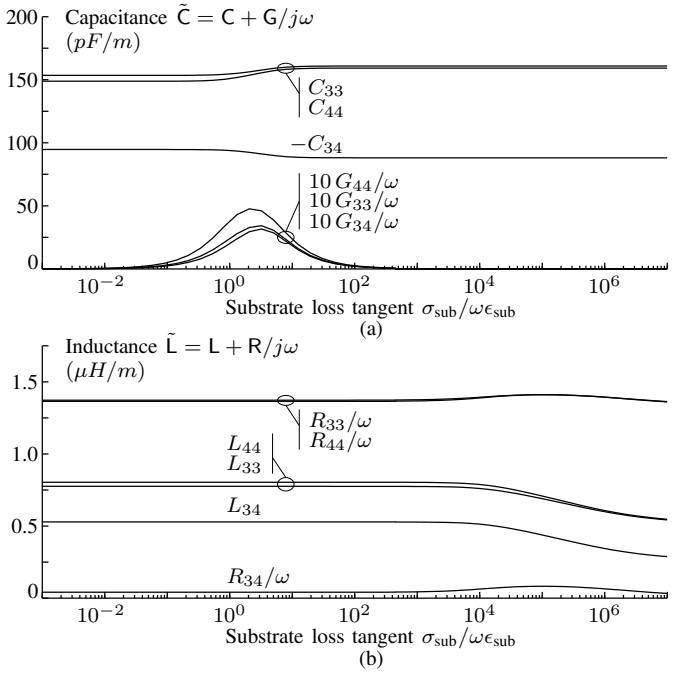

Fig. 9. Elements of complex capacitance matrix $\tilde{\mathsf{C}}$ and inductance matrix $\tilde{\mathsf{L}}$ for the structure of Fig. 6 at 10 GHz, as a function of the substrate loss factor. (a) Entries of $Re(\tilde{\mathsf{C}}) = \mathsf{C}$, compared to $-Im(\tilde{\mathsf{C}}) = \mathsf{G}/\omega$ (scaled by a factor 10 for clearness), and (b) elements of $Re(\tilde{\mathsf{L}}) = \mathsf{L}$, compared to $-Im(\tilde{\mathsf{L}}) = \mathsf{R}/\omega$.

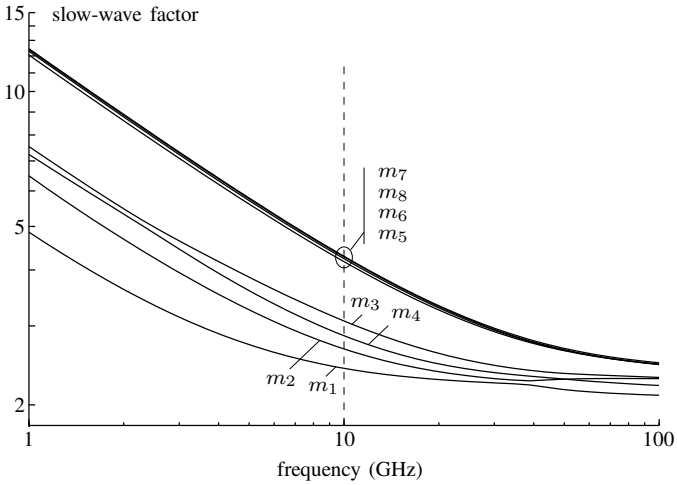

Fig. 10. Slow-wave factor as a function of frequency for the fundamental modes m_1 to m_8 of Fig. 6 (with $\sigma_{\text{sub}} = 2\,S/m$). The dotted line denotes the frequency at which the modal voltages are shown in Fig. 2.

$(C_s - |C_m|)$. Furthermore, $|j\omega L_s + R_s|$ is considerably higher than $|j\omega L_m + R_m|$, due to the large line resistance R_m, see Fig. 9(b). Going back to (3), the above considerations immediately lead to the observed difference in magnitude of the SWF of the even and odd modes.

Similar reasonings can be put forward to explain the attenuation constants. The main effect is here that the odd modal currents, opposite in both conductors of each pair, tend to repel each other, and hence flow through a smaller effective area of the conductors than the currents of the even modes, resulting in a higher attenuation.

The conductance coefficients G_{33}, G_{34} and G_{44} shown on Fig. 9(a), clearly demonstrate the semiconductor's behavior. For a very low conductivity σ_{sub}, $\mathbf{e}_t$ must be taken into account but the transverse currents $\sigma_{\text{sub}}\mathbf{e}_t$ are still negligible. When σ_{sub} increases, the transverse currents and the G-values also increase. However, as soon as the loss tangent becomes considerably higher than 1, charge relaxation reduces $\mathbf{e}_t$. This effect outweighs the increase in σ_{sub} and hence the G-values decrease again and in the end become negligible as soon as the substrate's surface potential has become constant.

Finally, the frequency-dependency of the SWF is shown in Fig. 10, for a substrate conductivity $\sigma_{\text{sub}} = 2\,S/m$. The transition from the *RC-* to the *LC-range* takes place around 20 GHz. This frequency is quite high because the conductors' cross-sections are small, resulting in large R-values.

REFERENCES

[1] F. Olyslager, *Electromagnetic Waveguides and Transmission Lines*. Oxford, U.K.: Oxford Univ. Press, 1999.

[2] G. Plaza, R. Marques, and F. Medina, "Quasi-TM MoL/MoM approach for computing the transmission-line parameters of lossy lines," *IEEE Trans. Microwave Theory Tech.*, vol. 54, no. 1, pp. 198–209, Jan. 2006.

[3] D. De Zutter and L. Knockaert, "Skin effect modeling based on a differential surface admittance operator," *IEEE Trans. Microwave Theory Tech.*, vol. 53, no. 8, pp. 2526–2538, Aug. 2005.

[4] T. Demeester and D. De Zutter, "Quasi-TM transmission line parameters of coupled lossy lines based on the Dirichlet to Neumann boundary operator," *IEEE Trans. Microwave Theory Tech.*, vol. 56, no. 7, pp. 1649–1660, july 2008.

[5] ——, "Modeling the broadband inductive and resistive behavior of composite conductors," *IEEE Microwave Wireless Compon. Lett.*, vol. 18, no. 4, pp. 230–232, Apr. 2008.

[6] "Compact modeling of on-chip passive structures at high frequencies," IST-2001-34058 project.

Daniël De Zutter was born in 1953. He received his M.Sc. Degree in electrical engineering, Ph.D. degree, and a thesis leading to a degree equivalent to the French Aggrégation or the German Habilitation from Ghent University, Ghent, Belgium, in 1976, 1981, and 1984, respectively.

From 1984 to 1996 he was with the National Fund for Scientific Research of Belgium. He is currently a Full Professor of electromagnetics with Ghent University. Most of his earlier scientific work concerned the electrodynamics of moving media. His research currently focuses on all aspects of circuit and EM modeling of high-speed and high-frequency interconnections and packaging, EM compatibility, and numerical solutions of Maxwell's equations. He has authored or coauthored over 140 international journal papers and 150 papers in conference proceedings.

He was the recipient of the 1999 Transactions Prize Paper Award presented by the IEEE Electromagnetic Compatibility (EMC) Society. In 2000 he was elected to the grade of Fellow of the IEEE. In the past 4 yeas he served as dean of the Faculty of Engineering of Ghent University. He is an associate editor for the MTT-Transactions.

Thomas Demeester was born in Ghent, Belgium, in 1982. He received the M.Sc. Degree in electrical engineering from Ghent University, Ghent, Belgium, in 2005, and is currently working toward the Ph.D. degree at Ghent university.

He spent one year with ETH Zürich, where he was involved in the field of time-domain electromagnetics. He is currently a Research Fellow of the Fund for Scientific Research (FWO-V), Flanders, Belgium. His research concerns electromagnetic field calculations in the presence of highly lossy media, and the development of transmission line models for interconnects.

VI Iberian Meeting on Computational Electromagnetism
(VI Encuentro Ibérico de Electromagnetismo Computacional, VI EIEC)
22-24 October 2008, Chiclana de la Frontera (Cádiz, Spain)
II LEMA-EPFL Workshop on Integral Techniques for Electromagnetics

21 October 2008, Chiclana de la Frontera (Cádiz, Spain)

PROGRAM VI EIEC

INVITED TALKS

As in the previous issue, Aiguablava (Girona), the "VI Iberian Meeting on Computational Electromagnetics" will include a number of invited talks given by prestigious international experts. At the moment, the following invited speakers have confirmed their contributions:

- Prof. Dr. Daniël De Zutter , Electromagnetics Group, Faculty of Engineering, Universiteit Gent (Belgium). Dean of the Faculty of Engineering.
  Title: *"Transmission Line Modeling of Coupled Lines in a Semiconducting Substrate"*
  Authors: *Daniël De Zutter and Thomas Demeester.*